Delayed Alpha Emission from Na^{20}†

R. M. Polichar,* J. E. Steigerwalt, J. W. Sunier, and J. Reginald Richardson
University of California, Los Angeles, California
(Received 22 May 1967; revised manuscript received 27 July 1967)

The β decay of Na^{20} proceeding to highly excited states of Ne^{20} has been studied by measuring the delayed α particles which are subsequently emitted. Na^{20} was produced by a $(p,\alpha n)$ reaction on a natural magnesium target, in an external beam of 45-MeV protons from the UCLA cyclotron. A thin silicon detector and nanosecond electronics were used to suppress the large positron background usually present in this type of experiment. A method of measuring Q_α directly is discussed. α transitions from states in Ne^{20} at 7.43, 7.84, 8.74, 9.48, 10.28, 10.86, and 11.28 MeV have been observed and their intensities measured.

1. INTRODUCTION

ALTHOUGH a number of studies have been made on Na^{20} since its discovery in 1950 by Alvarez,[1] until recently little more has been known than its half-life and approximate mass, based on a single positron transition. Moreover, the relative ground-state mass deduced from these earlier studies was higher than one would predict from Coulomb energy and isospin systematics. While the question of this apparent mass discrepancy has now been resolved both by nuclear reaction experiments[2,3] and by measurement of the β spectrum,[4] there is still considerable interest in knowing the properties of the very weak β decays which proceed to highly excited states in Ne^{20}. In this work we have indirectly measured the Na^{20} decay scheme by studying the delayed α spectrum resulting from these positron transitions. Of particular importance are those β transitions to $T=1$ levels in Ne^{20} which violate isospin in their subsequent α emission.

The delayed emission of a heavy particle following β decay is energetically possible whenever the mass of the level, populated by the β decay, is greater than the mass of two or more composite fragments. While, generally speaking, delayed heavy-particle measurements provide similar information to conventional β- and γ-ray spectroscopy, there are certain advantages and simplifications to be gained by these measurements. As a rule, if particle emission can take place, it will strongly dominate any radiative decay from the same level. This means that one can use the relative intensities of the particle lines to measure the relative strengths of β transitions which precede them. The spectrum of heavy particles consists of discrete lines which can be easily detected and identified. This makes accurate energy and intensity determinations easier and allows one to indirectly detect weak β transitions which would go undetected in conventional spectroscopy. The number of states to which a given level can decay by heavy-particle emission is somewhat limited, and there are no cross-over lines to contend with, which makes the assignment of the level scheme much easier. Finally, because of the combination of strong selection rules in both the β decay and the subsequent heavy-particle emission (especially for α particles) one can often make unambiguous spin and parity assignments just by finding the presence of a given transition.

The β-delayed α emission from Ne^{20} is an unusually interesting case to study. The Na^{20}-Ne^{20} mass difference is 13.90 MeV, and Ne^{20} has an extremely low α separation energy of 4.73 MeV. Between these limits, a number of levels satisfy the spin and parity requirement (2^+) for population by allowed β decay and subsequent α emission. By comparing the data obtained from the β- and α-ray spectroscopy of the type described, one hopes to understand the connection of the ground state of Na^{20} with the various excited states populated in Ne^{20} as well as the intrinsic structure of these excited states.

During the course of this work MacFarlane and Siivola[5] published their results on the delayed α emission from Na^{20}. In their work Na^{20} was produced via a complex reaction using a Ne^{20} ion beam and a number of targets. Because of the large differences in the approach to the problem, and of the fact that some questions were left unanswered, it was felt worthwhile to finish this study.[6] We have identified three additional transitions. In addition, we have developed a method to measure directly the Q value for α decay. This method makes use of the recoil energy imparted to the delayed α emitter by the nuclear reaction used for its production. This energy is sufficient to project it into the sensitive volume of the detector, where the sum of the energies of the α particle and of the O^{16} recoil ion is then measured.

2. EXPERIMENTAL PROCEDURES

The present experiments were carried out using an external beam of 45-MeV protons from the UCLA Spiral Ridge cyclotron. Na^{20} was produced by $(p,\alpha n)$ reaction on a natural, spectroscopically pure, magnesium target.

† Supported in part by the U. S. Office of Naval Research under Contract Nonr 233-44.
† Present address: University of Michigan, Cyclotron Laboratory, Ann Arbor, Michigan.
[1] L. W. Alvarez, Phys. Rev. **80**, 519 (1950).
[2] P. F. Donovan and P. D. Parker, Phys. Rev. Letters **14**, 147 (1965).
[3] R. H. Pehl and J. Cerny, Phys. Letters **14**, 137 (1965).
[4] J. W. Sunier, A. J. Armini, and J. R. Richardson, following paper, Phys. Rev. **163**, 1091 (1967).
[5] R. D. MacFarlane and A. Siivola, Nucl. Phys. **59**, 168 (1964).
[6] R. M. Polichar, Ph.D. thesis, UCLA, 1966 (unpublished).

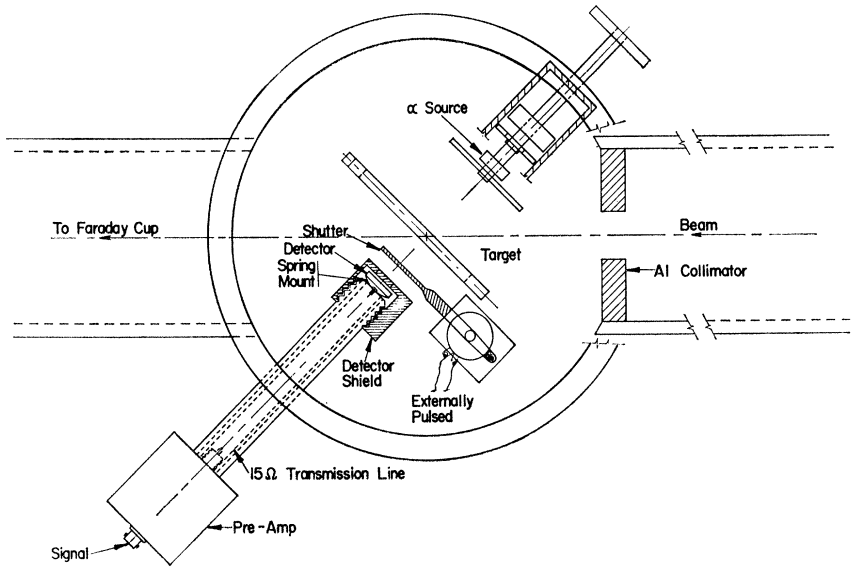

FIG. 1. Internal arrangement of vacuum chamber and detector system for direct α and absorbed recoil spectra.

The arrangement of the vacuum chamber used for the bombardments is shown in Fig. 1. The beam spot on the target was approximately $\frac{3}{8}$ in. in diameter with a typical beam current of 0.5 to 1 μA. The solid-state detector system and the associated electronics, which will be described elsewhere,[7] were designed to suppress the large electron background and pulse pileup which are usually present in this type of experiment. The electronics used the principle of fast gating and stretching suggested by Katzenstein[8] and allowed energy threshold discrimination of pulses with a pulse pair resolution of 12–14 nsec. This short time constant reduced the pulse pileup distortion to a completely negligible amount.

The beam was keyed on and off by pulsing the cyclotron oscillator in bursts of 0.5 to 3 sec. The cycling of the cyclotron's oscillator and the associated counting equipment was controlled by a multichannel digital sequence timer. In addition to conventional pulse-height analysis, some of the data were fed into an SDS 925 computer, where a time analysis of the pulse-height spectrum was performed, under control of the sequence timer. The half-life of the delayed α transitions was measured to be 0.41 ± 0.01 sec. A small contamination, resulting from delayed α emission from Al^{24} and B^{8} produced on the target was observed in the low-energy portion of the α spectrum.

The energy spectrum of the emitted α particles was studied in three ways. The first method was simply to look at the direct α radiation produced by the Ne^{20} formed in the target as one does in conventional α-ray spectroscopy. For this type of measurement, extremely thin targets are desirable but in practice one must settle for a compromise between reasonable counting rates and the broadening of the resolution produced by target thickness. A target thickness of 1μ proved to be optimum in our experiment. The primary virtue of the method is that it is simple and direct, and that the counter efficiency and solid angle are not dependent on the α energy.

As the experiment progressed, we developed a second method: to study the total energy spectrum of the breakup of the Ne^{20} ions absorbed within the solid-state detector itself. One can easily calculate what the maximum energy of the Na^{20} ion produced by a $(p,\alpha n)$ reaction would be in our case. For this, we assume that the α and neutron come off together in the backward (180°) direction. The Na^{20} ion emitted at 0° gets a maximum energy of about 6 MeV, taking into account the energy of the incident proton (45 MeV) and the Q value of the Mg^{24} $(p,\alpha n)$ reaction (−24.1 MeV). If one extrapolates from data of Northcliff[9] and Poskanser[10] on the range of Ne and Na ions in aluminum, one can make an estimate of the range of the recoiling Na^{20} ion in our silicon detector. This turns out to be 4.2 μ for the most energetic Na^{20} ion.

The process is shown schematically in Fig. 2. The recoil Na^{20} ion from the target enters the detector through the thin gold layer (thickness equivalent to 0.1 μ of silicon), β decays to Ne^{20} which then immediately breaks up into an α particle and a residual O^{16} ion. There is a good probability that the O^{16} ion will not have enough energy to escape, and the entire decay energy will be dissipated in the sensitive volume of the detector. Since the source is inside the detector, there are no target thickness effects, and because one measures the total decay energy, one can make a consistency check for a given line to see that it corresponds to the decay

[7] R. M. Polichar and J. E. Steigerwalt (to be published).
[8] H. S. Katzenstein, IEEE Trans. Nucl. Sci. NS-13, 527 (1966).
[9] L. C. Northcliff, Phys. Rev. 120, 1744 (1960).
[10] A. M. Poskanzer, Phys. Rev. 129, 385 (1963).

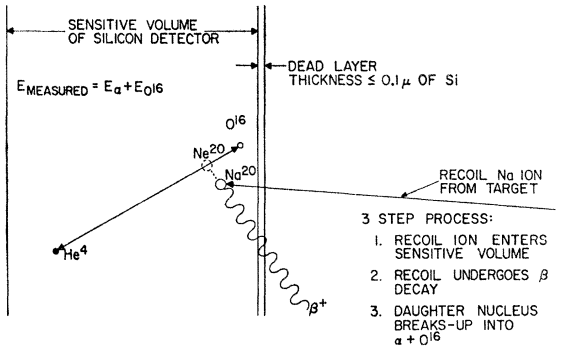

FIG. 2. Mechanism involved in the absorbed recoil-ion spectrum.

of a mass-20 nucleus. The disadvantage of the technique is that one cannot directly measure the relative intensities of lines of different energies. Both the energy distribution of the incoming Na^{20} ions and the varying O^{16} range for each transition contribute to a continuum, which must be subtracted from the spectrum. The total capture efficiency drops sharply with increasing α energy.

Obviously, if precautions are not taken, one will see both direct and absorbed recoil spectra in a spectrum taken with a simple detector looking directly at the target. To prevent this mixing, a shutter of 5-mil copper was placed between the target and the detector. The shutter could then be switched open or closed so as to either protect the detector from recoils during bombardment and see the direct α radiation during the counting period, or conversely, allow the recoils to penetrate during bombardment and block the view of the target during counting. The counter angle was also changed to either enhance or suppress the recoil production.

A third type of measurement was made which combined the characteristics of the first two. Recoils from a relatively thick (0.5-mil) magnesium radiator foil were allowed to strike a clean silver-leaf catcher foil placed at the normal target position. By placing the counter at 135° it was possible to measure the direct α spectrum from the decaying recoil ions caught on the silver leaf

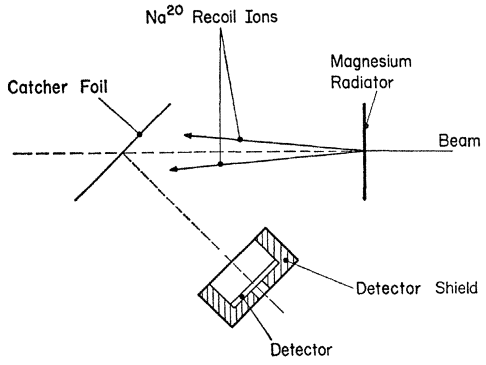

FIG. 3. Schematic layout of the detection system used with the catcher foil technique.

without appreciable contribution from direct radiation from the magnesium foil. A schematic layout of the target and detector system used in this case is presented in Fig. 3. The thickness of the catcher foil was 200 $\mu g/cm^2$. Since the counting rate for this method was much less than that for either of the first two techniques, the background played a much larger role and made it difficult to get quantitative information on all peaks. However, since the effective target thickness was extremely small, it cleared up several ambiguities among some of the weak or closely placed α groups.

3. EXPERIMENTAL DATA

3.1 Absorbed Na^{20} Recoil Data

To study the absorbed recoil-ion breakup, we opened the shutter in front of the detector in phase with the cyclotron beam burst. The detector was placed at 45° to enhance the recoil absorption process. A typical spectrum of the absorbed recoil-ion spectrum is shown in Figs. 4(a) and 4(b). Looking at the general shape of the spectrum, one sees that although the background continuum produced by incomplete absorption of the total energy is quite high, it by no means destroys the structure of the peaks or causes a significant broadening in the resolution. The principal disadvantage of the method is that the relative efficiency of the process drops with increasing α energy and must be calibrated if one is to extract meaningful intensities from the spectrum. The lines at 2.70, 3.12, 4.75, 5.55, 6.15, and 6.60 MeV have been identified as coming from states in Ne^{20}. In addition, there is some indication of a line at approximately 4.1 MeV which, although quite obscure in the recoil spectrum, shows up in other data taken. The broad peak at approximately 1.7 MeV comes from Al^{24} produced in the same target by the reaction $Mg^{24}(p,n)Al^{24}$.

3.2 Direct α Data

A typical direct α spectrum is shown in Figs. 5(a) and 5(b). The energies shown are those measured and must be corrected for self-absorption of the target as well as kinematics. The lines at 2.05, 2.38, 3.10, 3.72, 4.38, 4.83, and 5.13 MeV have been identified as coming from Ne^{20} and correspond to the transitions observed in the absorbed recoil spectrum. The line at 1.4 MeV corresponds to the 1.7-MeV recoil line and comes from the delayed α emission of Al^{24}. The two sharp lines at 2.70 and 5.5 MeV are remnants of the absorbed recoil spectrum. Because of occasional malfunction of the shutter, we always found some leakage of recoil ions onto our detector during the direct α runs. Since the yield of the absorbed recoil process was as much as an order of magnitude higher than the direct spectrum, the mixing of reactions was always most noticeable in the direct spectra. To confirm this fact, we took a direct α spectrum, covering the detector with an absorber

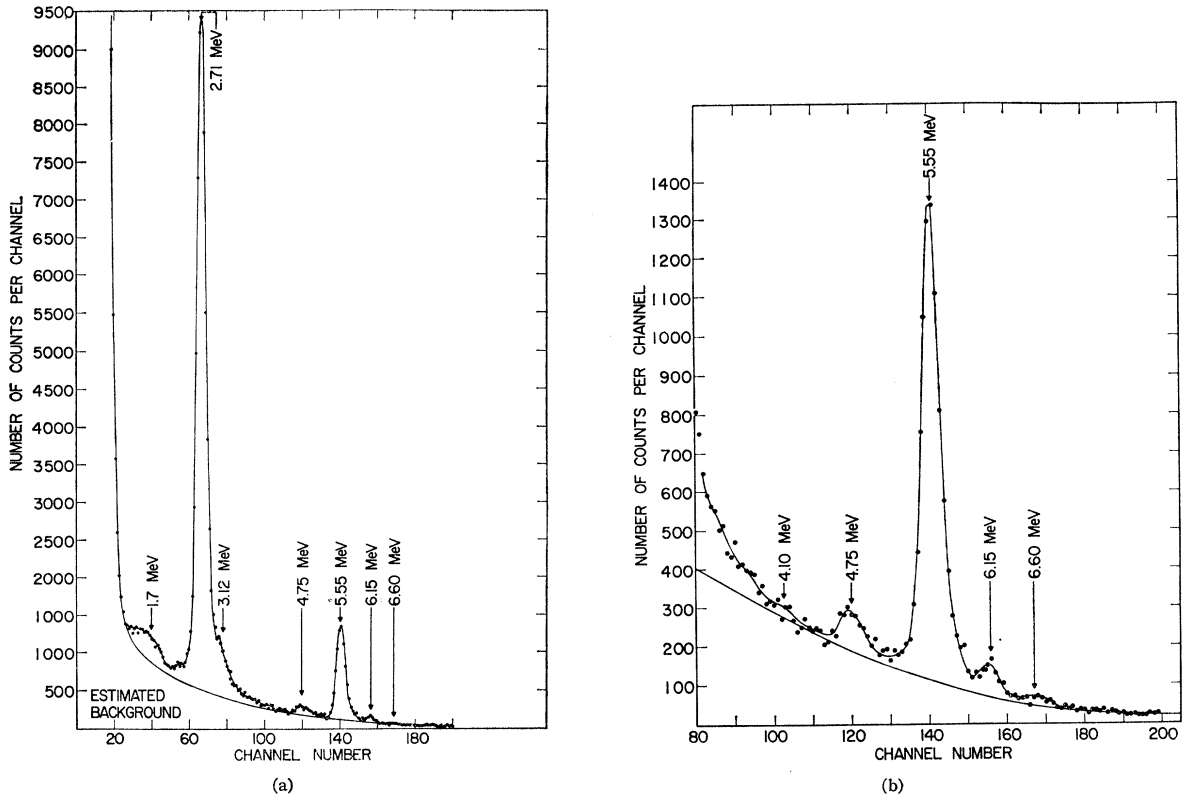

FIG 4. (a) Absorbed recoil breakup spectrum. (b) High-energy portion of absorbed recoil breakup spectrum.

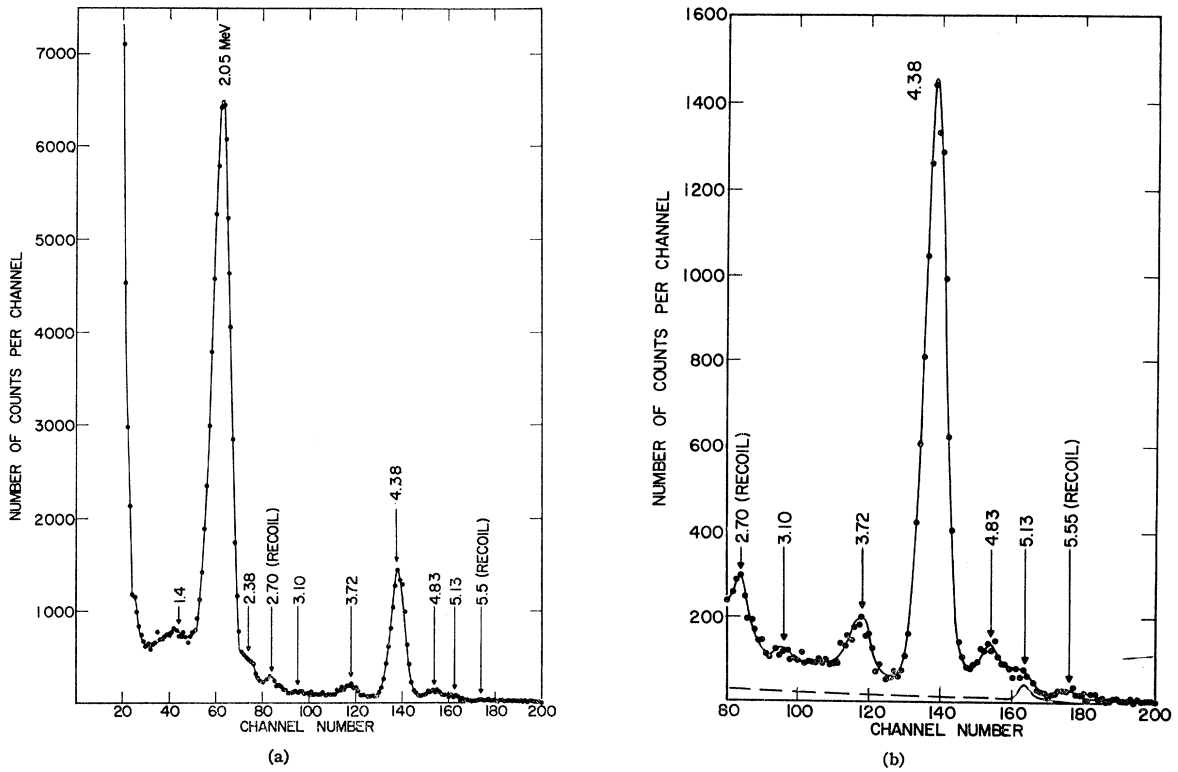

FIG. 5. (a) Direct α spectrum. (b) High-energy portion of the direct α spectrum.

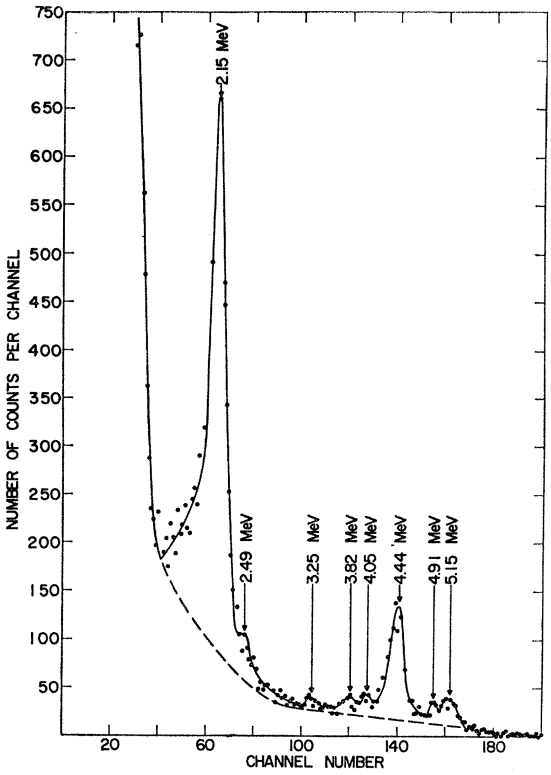

FIG. 6. α spectrum from a foil catching the Ne^{20} recoil ions emerging from a thick radiator.

thick enough to reduce the α energy by about 150 keV. The lines belonging to the direct α spectrum were reduced in energy, whereas the 2.7- and 5.5-MeV lines maintained the same energy but were much reduced in intensity.

In order to interpret the direct α spectra and obtain the energies and intensities, it is necessary to correct for target self-absorption. For our correction procedure, we assumed that the target was relatively thin so that, (a) the average energy loss was proportional to the target thickness and dE/dX for the corresponding incident α energy, and (b) the production of Na^{20} ions produced a symmetric distribution in the target having an effective thickness t, and hence produced a Gaussian spread in energies having a half-width just twice the average energy loss. Thus, the width of a given peak was given by the root-mean-square sum of the system noise and this calculated energy spread. All one needs to know then is the energy shift for one peak and, from a table of dE/dX, one can determine the normalizing constant and the effective target thickness, and predict the shift and spreads of the other peaks. In our case, there were two prominent peaks in both the recoil and direct spectra which could be related. For the data shown above, the effective thickness determined by this procedure was 210 ± 2 $\mu g/cm^2$ and the widths calculated on this basis agree very well with those measured. The rest of the lines in the spectra were then corrected using the same procedure with the determined value of t.

3.3 Catcher Foil Data

A typical spectrum is shown in Fig. 6. The yield of the catcher process was very low, primarily due to the two solid angles involved and to the fact that part of the recoil Na^{20} ions had sufficient energy to pass through the catcher foil. Consequently, the background was much higher than in the two other measurements discussed above. The line at 4.05 MeV and part of the line at 5.15 MeV are long lived and do not belong to the delayed α spectrum of Ne^{20}. Due to the very small effective target thickness, this spectrum gave the clearest evidence for the presence of the 2.49- and 3.25-MeV lines in the spectrum. The α energies obtained from this measurement agree very well with those obtained after target thickness corrections in the direct α data. (See Table I).

4. ANALYSIS OF THE DATA

In order to calculate the intensities and energies from the raw spectra, it was necessary to substract the background. In the case of the direct α spectra, this background was a composite of electron multiple scattering in the low-energy regions and an almost smooth distribution of heavy-particle background arising from the target. Spectra were taken with uncoated silver backing foils which gave an estimate of the electron background. Impurities in the magnesium itself (especially carbon) and perhaps several other very weak Na^{20} transitions consititute the rest of the background. Pulse pileup and other intensity-dependent spectral distortions, which often are a problem in delayed heavy-

TABLE I. Direct α data.

α_i	E_α(MeV) "Measured"	Correction $\Delta\epsilon(E)$	E_α(MeV) "Corrected"	Q_α(MeV)	Corresponding level in Ne^{20}	Relative intensity
α_1	2.05±0.01	0.110±0.006	2.16±0.01	2.70±0.01	7.43±0.01	100.0
α_2	2.38±0.03	0.100±0.005	2.48±0.03	3.10±0.04	7.83±0.04	4.0
α_3	3.10±0.03	0.086±0.004	3.18±0.03	3.98±0.04	8.71±0.04	0.3
α_4	3.72±0.02	0.078±0.003	3.80±0.02	4.75±0.03	9.48±0.03	1.4
α_5	4.38±0.01	0.071±0.003	4.45±0.01	5.56±0.02	10.29±0.02	17.0
α_6	4.83±0.02	0.066±0.003	4.90±0.02	6.13±0.03	10.86±0.03	1.2
α_7	5.13±0.04	0.064±0.003	5.19±0.04	6.49±0.05	11.22±0.05	0.6

particle measurements, are negligible using our present electronics system.

The absorbed recoil data were complicated even further by the large low-energy tail created by the incomplete absorption of both the α and the recoil O^{16} ion. It was determined experimentally that at least half of the events in the high-energy region of the spectrum fall outside the well-defined peaks and contribute to the general background.

In both cases several combinations of effective backgrounds were tried, to arrive at the best over-all line shapes consistent with our known target thickness and system resolution. It should be pointed out that all reasonable choices of background produced only small changes in the intensities of the high-energy peaks and really only made significant changes for the intensity of the 2.49- and 3.21-MeV α lines of the low-energy region. After the background subtraction, we have approximated Gaussian distributions to the data points, adjusting the tails of the larger peaks to produce the calculated width for the neighboring smaller peaks.

Table I gives a summary of the energies and intensities deduced from the direct α data. The target corrections shown are typical for all the data taken. In the table the intensity of the 2.16-MeV line has been taken to be 100. The lines are designated $\alpha_1 \cdots \alpha_7$ in order of increasing energy and include only what we believe correspond to transitions from Ne^{20}.

Table II gives the summary of the energies and the relative intensities of the absorbed recoil lines. In combining data from all the techniques used in the experiment, one can estimate fairly well the consistency of the data. The fact that the α energy measured in the lab is related in a simple way to the total decay energy measured in the absorbed recoil technique provides a check on the origin of each line. All the lines, with the exception of α_3, are clearly visible in both types of spectra. Since the intensity of this line is so weak, it could well have been lost in the background of the absorbed recoil experiments. The fact that it was determined to be an α by dE/dX measurements and that its relative intensity did not vary much with different counting times leads us to believe it has the same half-life as the other lines and most probably belongs in the Na^{20} decay scheme.

TABLE II. Na^{20} absorbed recoil data.

α_i	E_{recoil} (MeV)	Corresponding level in Ne^{20}	Relative intensity
α_1	2.70±0.01	7.44±0.01	100.0
α_2	3.12±0.04	7.85±0.04	5.5
α_4	4.75±0.03	9.48±0.03	1.0
α_5	5.55±0.02	10.28±0.02	11.1
α_6	6.15±0.03	10.88±0.03	0.65
α_7	6.60±0.05	11.33±0.05	0.22

Table III gives a combined data summary for all the experimental data. The values for E_α are taken from both direct α runs as well as the catcher foil experiment and our best values of the true lab energy after target corrections. The recoil values represent best values for the absorbed recoil experiments. The excitation energy of the corresponding levels in Ne^{20} were computed from weighted averages of all these data.

The final values for the relative intensities have been taken for the most part from the direct α data, since they do not depend on the α energy. The two exceptions to this procedure were for α_2 and α_7. In the case of α_2 both the uncertainty in the actual background as well as the difficulty in resolving and unfolding the direct α_2 line from the very intense α_1 line lead to a rather low-intensity value when compared to the absorbed recoil data. Since α_1 and α_2 are so close in energy we might well expect to see the same ratio in both types of experiment or perhaps a reduction in the absorbed recoil data. The value given is the average of the two types of experiments and is probably slightly too low. The α_7 line in the direct α spectrum was obscured by a long-lived contaminant at 5.2 MeV so it was necessary to extrapolate the efficiency of the absorbed recoil method to this energy and then correct the intensity measured in that experiment to get its true intensity. This was done by extrapolating the ratio of I recoil/I direct for α_4, α_5, and α_6.

The principal source of error in the measurement of relative intensities was in the subtraction of the background. Estimates of this error, assuming reasonable

TABLE III. Combined data summary.

α_i	E_α[a]	E_{recoil}[b]	Deduced level in Ne^{20}[c]	"Known" level in Ne^{20}[d]		Relative intensity
α_1	2.16±0.01	2.70±0.01	7.43±0.01	7.43	2^+	100.0
α_2	2.49±0.02	3.12±0.04	7.84±0.03	7.84	2^+	4.7±0.9
α_3	3.21±0.03	···	8.74±0.03	8.73	(1^-)	0.3±0.1
α_4	3.81±0.02	4.75±0.03	9.48±0.02	9.50	2^+	1.4±0.1
α_5	4.44±0.01	5.55±0.02	10.28±0.01	10.27	2^+	17.0±0.8
α_6	4.90±0.02	6.15±0.03	10.86±0.02	10.83	2^+	1.2±0.2
α_7	5.14±0.03	6.60+0.05	11.28±0.04	11.27	2^+	0.4±0.1

[a] From direct α and catcher foil data.
[b] From absorbed recoil data.
[c] Weighted averages from all data in this experiment.
[d] From Ref. 11 and J. D. Pearson, E. Almqvist, and J. A. Kuehner, Can. J. Phys. 42, 489 (1964).

variations in the shape and intensity of the background, suggest that for the two cases discussed above, the error might be as large as 20%, but for the other lines 10% seems to be a conservative limit. This can make only a very small change in the interpretation of the nature of the β decay involved.

5. COMPARISON WITH OTHER WORK AND CONCLUSION

The observed α decay and the corresponding levels in Ne^{20} are shown in Fig. 7. The energy values deduced for the Ne^{20} levels agree with the data compiled by Ajzenberg–Selove and Lauritsen.[11] The relative intensities and the energies of the observed α transitions agree quite well with the data of MacFarlane and Siivola.[5] These authors did not observe lines corresponding to our α_3, α_6, and α_7, mainly because of their weak intensity. There is, however, some hint of a transition corresponding to our α_6 in their experimental spectrum.

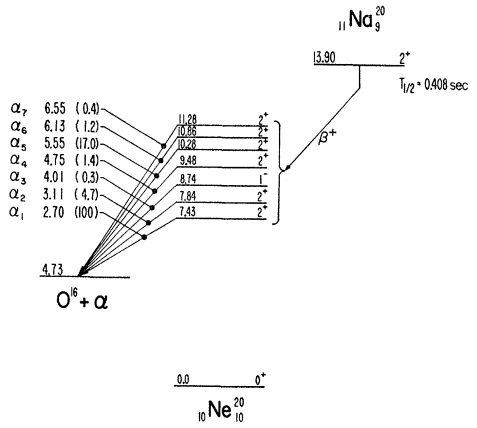

FIG. 7. Partial decay scheme of Na^{20} and β- delayed α transitions to O^{16}. The energies are given in MeV and the numbers in parentheses give the relative intensities of the transitions.

One of the primary reasons for doing delayed heavy-particle studies is to determine indirectly intensities and energies of β transitions. Some of these branches are so weak that it would be extremely difficult, if not impossible, to detect them from the techniques of conventional β spectroscopy. One of the drawbacks of these indirect investigations is that they cannot give absolute β-transition probabilities, because only the β transitions which happen to feed particle unstable levels can be observed. Although it has been common practice to estimate the *ft* value of one particular β transition (usually the superallowed transition between analog states), and to use this value to compute the others from the relative intensities obtained from delayed-particle studies, we feel that this procedure might be misleading. The main argument is that the β transition used for this "semiempirical" normalization might just be abnormally fast or slow, in which case some interesting detail aspects of nuclear structure would go undetected. Accurate information on the β decay leading to a delayed particle emitter can only be obtained if a direct β-spectrum measurement can establish a link to at least one particle unstable state. In the particular case of Na^{20}, such a link has been studied[4] and will allow us to make full use of the information reported in this work.

ACKNOWLEDGMENTS

We wish to thank Dr. H. Katzenstein and Dr. F. Ziemba for their assistance in developing the detector electronics system, and Dr. A. J. Armini for his suggestions and help during the runs. We are indebted to the cyclotron crew for their help in running the cyclotron.

[11] F. Ajzenberg-Selove and Y. Lauritsen, in *Nuclear Data Sheets*, compiled by K. Way *et al.* (U. S. Government Printing Office, National Academy of Sciences—National Research Council, Washington 25, D. C.), NRC 61-5,6-307.